Scattering of Plasmons at the Intersection of Two Metallic Nanotubes: Implications for Tunneling

V. V. Mkhitaryan, Y. Fang, J. M. Gerton, E. G. Mishchenko, and M. E. Raikh
Department of Physics, University of Utah, Salt Lake City, Utah 84112, USA
(Received 27 June 2008; published 18 December 2008)

We study theoretically the plasmon scattering at the intersection of two metallic carbon nanotubes. We demonstrate that, for a small angle of crossing $\theta \ll 1$, the transmission coefficient is an oscillatory function of λ/θ, where λ is the interaction parameter of the Luttinger liquid in an individual nanotube. We calculate the tunnel density of states $\nu(\omega, x)$ as a function of energy ω and distance x from the intersection. In contrast with a single nanotube, we find that, in the geometry of crossed nanotubes, conventional "rapid" oscillations in $\nu(\omega, x)$ due to the plasmon scattering acquire an aperiodic "slow-breathing" envelope which has λ/θ nodes.

DOI: 10.1103/PhysRevLett.101.256401 PACS numbers: 71.10.Pm, 72.15.Nj, 73.40.Gk

Introduction.—By now, observation of Luttinger liquid in 1D systems has been reported for single-walled carbon nanotubes [1–6] and GaAs-based semiconductor wires [7]. Conclusions about Luttinger liquid behavior have been drawn from analysis of the data, which can be divided into two groups: (i) power-law, $\propto (\max\{V, T\})^{\alpha}$, behavior of tunnel or source-drain conductance [1–6], where parameter α is the measure of deviation from the Fermi liquid behavior, and (ii) momentum-resolved tunneling in a parallel magnetic field [7].

On the conceptual level, the difference between techniques (i) and (ii) is that (i) probes a single-point Green function $\mathcal{G}(x, x, \omega)$, while (ii), by mapping $\int dx \int dx' \mathcal{G}(x, x', \omega) \exp[-iq_B(x - x')]$, with q_B proportional to applied field, yields information about a two-point Green function and thus is more informative.

With regard to quantitative determination of the Luttinger liquid parameter g, which is related to α as [8] $\alpha = (g^{-1} + g - 2)/8$, it is desirable to identify an effect, which would depend on g stronger than a power law. An example of such an effect was given by Ussishkin and Glazman in Ref. [9], where, due to electron backscattering, g appears in the argument of sine; this sine describes the amplitude modulation of the probe-induced Friedel oscillations [10], $\propto \cos(2k_F x)$ in the local density of states; k_F is the Fermi momentum.

In the present Letter, we demonstrate that the geometry of the crossed nanotubes (see Fig. 1) offers a qualitatively new manifestation of the Luttinger liquid behavior. In particular, the oscillatory dependence on g, similar to that in Ref. [9], emerges in the geometry of crossed nanotubes even without electron backscattering [5,11–13]. More precisely, we show that, in this geometry, the envelope, "breathing" with g, modulates not $\cos(2k_F x)$ oscillations but much slower oscillations resulting from the plasmon backscattering.

There is an important difference between scattering of plasmons and electrons: For an obstacle bigger than k_F^{-1}, electron scattering is exponentially suppressed, while plasmon scattering is efficient as long as the size of the obstacle does not exceed the plasmon wavelength. This scattering gives rise to the oscillations of the local density of states $\delta\nu(\omega, x) \propto \cos(2\omega x/v_F)$, where v_F is the Fermi velocity. It is these oscillations that acquire a breathing envelope in the geometry of crossed nanotubes (Fig. 2). Our main finding is that, with regard to this modulation, making the crossing angle θ small effectively enhances the Luttinger liquid parameter. To describe this enhancement quantitatively, we first consider an auxiliary problem of plasmon scattering at the intersection and later utilize it for the calculation of $\delta\nu(\omega, x)$.

Plasmon scattering at the intersection.—Assume that d is the minimal distance between the nanotubes. Even in the absence of electron tunneling, a plasmon propagating towards $x = 0$ in nanotube 1 can (i) pass $x = 0$ (transmission), (ii) excite a plasmon in nanotube 2, which propagates away from the intersection $x = 0$ either to the left or to the right (deflection), and (iii) get reflected. Incorporating the plasmon scattering into the formalism of the Luttinger liquid gives rise to the breathing envelope in Fig. 2. The underlying reason is that the interaction between the tubes strengthens towards intersection [14]. This leads to the x-dependent splitting of velocities in each tube. The resulting x-dependent phase accumulation near the intersection translates into nontrivial dependence of $\delta\nu(\omega, x)$. Moreover, the phase accumulation increases rap-

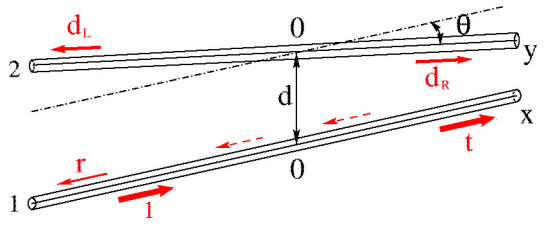

FIG. 1 (color online). Intersecting nanotubes, separated by a distance d; the angle of intersection is θ. Directions of incident, reflected r, transmitted t, and deflected d_L and d_R plasmon waves are shown with solid red arrows. Dashed arrows illustrate two contributions to the reflected wave.

 © 2008 The American Physical Society

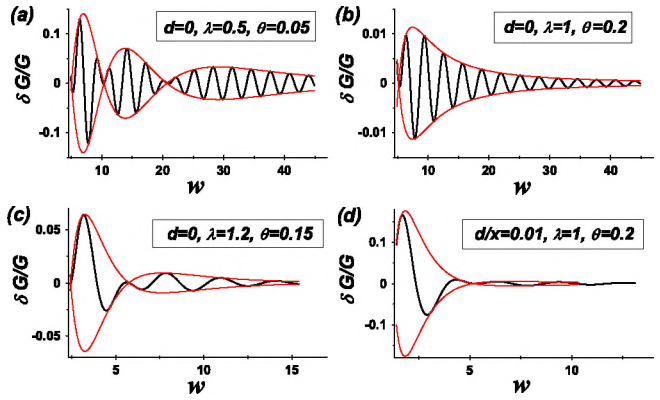

FIG. 2 (color online). Oscillating corrections to the tunneling conductance are plotted from Eq. (15) versus dimensionless bias $w = Vx/s$, where x is the distance from the intersection. Periodic oscillations (black line) are modulated by a breathing envelope (red line), with a period determined by λ/θ, where λ is the interaction parameter; (d) illustrates suppression of oscillations at finite separation $d = 0.01x$ between the nanotubes.

idly with decreasing angle θ, thus simulating the enhancement of the Luttinger parameter.

Collective modes of intersecting nanotubes.—As a result of long-range interaction $e^2 \int \frac{dxdx'}{|x-x'|} \frac{\partial u(x)}{\partial x} \frac{\partial u(x')}{\partial x'}$, where $u(x)$ is the displacement of the electron position from the equilibrium, the plasmon spectrum of an individual tube is $\omega(q) = qs(q)$ with velocity [8] $s = v_F[1 + \lambda \ln(qr)]^{1/2}$. Here r is the nanotube radius, and $\lambda = 8e^2/(\pi\hbar v_F)$ is the interaction constant [8]. Following Ref. [8], we neglect the relative change of $\ln(qr)$. At a given frequency ω, displacement $u(x)$ is the eigenmode $\hat{D}\{u(x)\} = (\omega^2/v_F^2)u(x)$ of the operator

$$\hat{D}\{f\} = -\frac{\partial^2}{\partial x^2} f(x) - \lambda \frac{\partial^2}{\partial x^2} \int_{-\infty}^{\infty} \frac{dy}{|x-y|} f(y). \tag{1}$$

For two crossed nanotubes, the eigenmodes are described by the system of two coupled equations

$$(\omega^2/v_F^2)u_{1,2}(x) = \hat{D}\{u_{1,2}(x)\} + \hat{F}\{u_{2,1}(x)\}, \tag{2}$$

$$\hat{F}\{f\} = -\lambda \frac{\partial}{\partial y} \int_{-\infty}^{\infty} \frac{dx}{\sqrt{d^2 + x^2 + y^2 - 2xy\cos\theta}} \frac{\partial f(x)}{\partial x}. \tag{3}$$

The operator $\hat{F}$ has a meaning of longitudinal force created by the density fluctuation $\partial u_1(x)/\partial x$ in nanotube 1, at point y of nanotube 2. The scattering problem corresponds to the solution of Eqs. (2) which has the following asymptotes at large x and y:

$$\begin{aligned} u_1(x)|_{x\to-\infty} &= e^{ikx} + re^{-ikx}, \qquad u_1(x)|_{x\to\infty} = te^{ikx}, \\ u_2(y)|_{y\to-\infty} &= d_L e^{-iky}, \qquad u_2(y)|_{y\to\infty} = d_R e^{iky}. \end{aligned} \tag{4}$$

Born approximation.—For small λ, the elements of scattering matrix can be found in the Born approximation in momentum space. To first order in λ, only d_R and d_L are nonzero. They are given by matrix elements of the operator $\hat{F}$ [Eq. (3)], namely, $d_R(k) = (i/2k)\hat{F}_{k,k}$ and $d_L(k) = -(i/2k)\hat{F}_{-k,k}$. The analytical expression for $\hat{F}_{p,q}$ is

$$\hat{F}_{p,q} = 2\pi\lambda \frac{pqe^{-(d/\sin\theta)(p^2+q^2-2pq\cos\theta)^{1/2}}}{(p^2+q^2-2pq\cos\theta)^{1/2}}. \tag{5}$$

This leads to the final result for deflection coefficients

$$d_R = i\pi\lambda \frac{e^{-kd/\cos(\theta/2)}}{2\sin(\frac{\theta}{2})}, \quad d_L = -i\pi\lambda \frac{e^{-kd/\sin(\theta/2)}}{2\cos(\frac{\theta}{2})}. \tag{6}$$

An apparent consequence of Eq. (6) is that deflection is exponentially small when the plasmon wavelength is $\ll d$. Less obvious is that, for $kd < 1$ and small θ, coefficients d_R and d_L can differ exponentially. This is because the exponent $\exp(-2kd/\theta)$ in d_L can be small if kd is small. Note that, in the long-wavelength limit $kd \ll \theta$, we still have $d_R/d_L \approx 1/\theta \gg 1$. The underlying reason is that d_L corresponds to the wave which travels almost in the opposite direction to the incident wave, while d_R travels almost along the incident wave. From Eq. (6) we conclude that the Born approximation applies at $\lambda \ll \theta$.

The reflection coefficient $r(k)$, in the second Born approximation, is expressed via the matrix elements [Eq. (5)]

$$r(k) = \frac{1}{4i\pi k} \int_{-\infty}^{\infty} \frac{dp}{p^2 - k^2 - i\epsilon} \hat{F}_{-k,p}\hat{F}_{p,k}. \tag{7}$$

The integral in Eq. (7) is the sum $(2\pi\lambda)^2 k(I_1 + iI_2)$ of contributions from the poles $p = \pm k$ and the principal value, which can be cast in the form

$$\begin{aligned} I_1 &= P\int \frac{dpp^2}{p^2-k^2} \frac{e^{-d/\sin\theta(p^2+k^2-2pk\cos\theta)^{1/2}}}{[(p^2+k^2)^2 - 4p^2k^2\cos^2\theta]^{1/2}} \\ &\quad \times e^{-d/\sin\theta(p^2+k^2+2pk\cos\theta)^{1/2}}, \\ I_2 &= \frac{\pi}{2\sin\theta} e^{-kd[1/\cos(\theta/2)+1/\sin(\theta/2)]}. \end{aligned} \tag{8}$$

For short wavelengths $kd \gg 1$, the dependence $r(k)$ is dominated by the integral $I_1 \approx -(\lambda^2/2) \times (kd\sin\theta/\pi)^{-3/2} e^{-2kd/\sin\theta}$. In the long-wavelength limit $kd \ll 1$, one can replace the exponent $e^{-kd/\sin\theta}$ by 1. In what follows, we will focus on small θ, where d_L and r diverge. Note that the pole contribution in Eq. (8) diverges for $\theta \to 0$ much stronger than the principal value contribution, which is $\propto \ln(1/\theta)$, so that $r \approx \pi^2\lambda^2/2\theta$. We also notice that, in the small-θ domain, the relation $r \approx d_L d_R$ holds. This relation can be understood from the following reasoning.

There are two contributions to the reflected wave in the second Born approximation. (i) The wave deflected into the second tube to the right with the amplitude (solid arrow in Fig. 1) undergoes a secondary deflection back into the first tube (dashed arrow in Fig. 1) with amplitude d_L. (ii) The wave deflected into the second tube to the left d_L is subsequently deflected back into the first tube with the ampli-

tude d_R (Fig. 1). The sum of the two contributions amounts to $r = (c_1 + c_2) d_L d_R$. Remarkably, both numerical factors c_1 and c_2 are equal to $1/2$. This is a consequence of a strong difference in distances at which formation of the primary left- and right-deflected waves takes place. The wave d_L is formed within $\sim 1/k$ from the intersection, while the wave d_R is formed within a much broader interval $\sim 1/(k\theta)$. Therefore, in the second tube, at some distance y from the intersection, such that $1/k \ll y \ll 1/(k\theta)$, the amplitude of the left-deflected wave is already d_L, while the amplitude of the right-deflected wave is only $\frac{1}{2} d_R$. Subsequent formation of contribution (ii) occurs at $y \sim 1/(k\theta)$, so that the corresponding amplitude is $(\frac{1}{2} d_R) d_L$, i.e., $c_2 = 1/2$. On the other hand, formation of contribution (i) takes place only over negative $-1/(k\theta) < y < 0$ and thus results in $d_L(\frac{1}{2} d_R)$, i.e., $c_1 = 1/2$.

Semiclassical description.—From Eq. (6) one can see that for $\theta < \pi\lambda$ the Born approximation renders an unphysical result, namely, $d_R > 1$, suggesting that this approximation is not applicable for small θ. This manifests the change in the mechanism of the plasmon scattering which takes place for $\theta \lesssim \lambda$. Indeed, at small θ, the incident wave travels closely to the wave d_R over a long distance, so that their amplitudes get mutually redistributed. Importantly, in describing this redistribution, one can (i) neglect both left-deflected d_L and reflected r waves and (ii) employ a semiclassical approach, which yields

$$t(k) = \cos\left(\frac{2\lambda}{\theta} \int_0^\infty dz K_0[\sqrt{k^2 d^2 + z^2}]\right),$$
$$d_R(k) = i \sin\left(\frac{2\lambda}{\theta} \int_0^\infty dz K_0[\sqrt{k^2 d^2 + z^2}]\right), \tag{9}$$

where K_0 is the MacDonald function. A remarkable feature of this result is that t and r oscillate strongly with θ and that the oscillations scale with the interaction constant. Note that, in the short-wavelength limit $kd \gg 1$, the perturbative result Eq. (6) is valid even for $\lambda > \theta$. Using the large-argument asymptote of $K_0(z)$, it is easy to see that Eq. (9) reproduces Eq. (6) in this limit. For the long-wavelength limit $kd \ll 1$, Eq. (9) yields $d_R = \sin(\pi\lambda/\theta)$, $t = \cos(\pi\lambda/\theta)$, so that the perturbative and semiclassical results match at $\lambda/\theta \lesssim 1$.

To outline the derivation of Eq. (9), we note that the system of equations (2) can be rewritten as two independent closed equations

$$(\omega^2/v_F^2) u_\pm(x) = \hat{D}\{u_\pm(x)\} \pm \hat{F}\{u_\pm(x)\}. \tag{10}$$

where combinations $u_\pm(x) = u_1(x) \pm u_2(x)$ are introduced. Searching for the semiclassical solution of Eq. (10) in the form $u_\pm(x) = e^{ikx + i\varphi_\pm(kx)}$, with slowly varying phase $\varphi'_\pm \ll 1$, we find

$$2\varphi'_\pm(kx) = \mp \lambda K_0\{[1 + \varphi'_\pm(kx)] k\sqrt{d^2 + x^2\theta^2}\}. \tag{11}$$

In evaluating the right-hand side, we assumed that θ is small. We see that when λ is small, the assumption $\varphi'_\pm \ll 1$ is justified. Then the smallness of $\varphi'_\pm$ allows one to neglect it in the argument of K_0. Upon integrating Eq. (11), we find $\varphi_\pm$. Then transforming back to u_1 and u_2, we recover Eq. (9). The expression for $r(k)$ generalized to the domain $\theta < \lambda < 1$ follows from Eqs. (6) and (9):

$$r(k)|_{\theta<\lambda} = d_R d_L = \frac{\pi\lambda}{2} e^{-2kd/\theta} \sin\left(\frac{2\lambda}{\theta} \int_0^\infty dz K_0[\sqrt{k^2 d^2 + z^2}]\right) \tag{12}$$

and in the long-wavelength limit simplifies to $r|_{\theta<\lambda} = (\pi\lambda/2)\sin(\pi\lambda/\theta)$.

Tunnel density of states.—Most importantly, the nontrivial dependence of the plasmon scattering on λ and θ manifests itself in the observables, e.g., in the dependence of tunnel density of states $\nu(\omega, x)$ on the distance x from the intersection. To illustrate this, consider first a single nanotube with inhomogeneity at $x = 0$ which scatters plasmons with reflection coefficient $\tilde{r}(k)$. Then the correction to the tunnel density of states reads

$$\frac{\delta\nu(\omega, x)}{\nu_0(\omega)} = \Gamma(\alpha + 1)\sqrt{\alpha^2 + \alpha/2} \frac{|\tilde{r}(\omega/s)|}{(2\omega x/s)^{\alpha+1}} \times \sin\left[\frac{2\omega x}{s} - \varphi(\omega/s) - \frac{\pi\alpha}{2}\right], \tag{13}$$

where $\varphi(k) = \arg(\tilde{r})$. Equation (13) follows from the expression for interaction contribution to the local Green function which takes into account the plasmon scattering:

$$\mathcal{G}(x, t) = \exp\left\{-\pi \int dk \left[\frac{|\int^x u_k|^2 sk}{8v_F} + \frac{|u_k(x)|^2 v_F}{8sk}\right] \times (1 - e^{-is|k|t})\right\}. \tag{14}$$

Here $u_k(x)$ are the plasmon eigenmodes: $u_k(x) = [e^{ikx} + \tilde{r}(k)e^{-ikx}]/\sqrt{2\pi}$ and $u_k(x) = \sqrt{(1 - |\tilde{r}|^2)/2\pi} e^{ikx}$ for $kx < 0$ and $kx > 0$, respectively. Expanding the exponent in Eq. (14) with respect to $\tilde{r}$, and evaluating $\nu(\omega, x) = \pi^{-1}\mathrm{Re}\int_0^\infty dt e^{i\omega t}\mathcal{G}(x, t)$, we arrive at Eq. (13).

Equation (14) emerges upon representing electrons via the dual bosonic fields $\theta_{i\alpha}$ and $\phi_{i\alpha}$, $\psi_{i\alpha} \sim e^{i(\phi_{i\alpha} \pm \theta_{i\alpha})}$; $i = 1, 2$ labels the two bands; $\alpha = \uparrow, \downarrow$ are the spins [8]. Interaction is completely described by the charged field $\theta_c = \frac{1}{2}\sum_{i\alpha}\theta_{i\alpha}$, while the three neutral sectors are noninteracting. Expansion [15] $\theta_c(x) = \pi\sqrt{n_0}\int dk u_k(x)\hat{Q}_k$, $\phi_c(x) = (1/\hbar\sqrt{n_0})\int dk[\int^x dy u_k(y)]\hat{P}_k$ over the plasmon eigenmodes $u_k(x)$ reduces the interacting Hamiltonian to a system of harmonic oscillators $\{\hat{Q}_k, \hat{P}_k\}$ yielding Eq. (14).

A simple reasoning allows one to generalize Eq. (13) to the case of two intersecting nanotubes. Indeed, with intersection playing the role of inhomogeneity, instead of one reflected wave with reflection coefficient $\tilde{r}$, we have two independent modes $u_\pm(x)$, solutions of Eq. (10), with reflection coefficients $r_\pm$. It is important that, while the absolute values r_+ and r_- are the same and equal to $|d_L|$, given by Eq. (6), their phases are different and are equal to

$\varphi_+(kx) - \varphi_+(-kx)$ and $\varphi_-(kx) - \varphi_-(-kx) + \pi$, respectively, where $\varphi_\pm$ are determined by Eq. (11). Because of this difference in phases, the oscillations $\propto \sin[2\omega x/s + \varphi]$ in Eq. (13) transform into a beating pattern

$$\frac{\delta\nu(\omega, x)}{\nu_0(\omega)} = -\Gamma(\alpha+1)\sqrt{\alpha^2+\alpha/2}\,\frac{\pi\lambda}{2}\,\frac{e^{-2\omega d/s\theta}}{(2\omega x/s)^{\alpha+1}} \times \sin\left(\frac{2\lambda}{\theta}\int_0^{\omega x\theta/s} dz K_0[\sqrt{(\omega d/s)^2+z^2}]\right) \times \cos\left(\frac{2\omega x}{s} - \frac{\pi\alpha}{2}\right). \quad (15)$$

Equation (15) is our main result. Remarkably, the shape of the envelope of $\cos(2\omega x/s)$ oscillations depends strongly on the interaction parameter λ, offering a unique signature of Luttinger liquid behavior. In particular, the number of nodes in the envelope is equal to λ/θ. Examples of oscillations Eq. (15) are plotted in Fig. 2 in terms of tunneling conductance $G(V, x) \propto \nu(\omega = V, x)$ for different interaction parameters. Note that the language of reflected plasmons r_+ and r_- applies at distances $x \gg s/V$, over which the reflection coefficient is formed. Since the characteristic scale of the envelope is $s/V\theta$, Eq. (15) is valid as long as $\theta \ll 1$. For large $x \gg s/V\theta$, the argument of the sine in Eq. (15) saturates at $\pi\lambda/\theta$. On physical grounds, the magnitude of the $\cos(2Vx/s)$ oscillations at large x should be given by Eq. (13), with element of scattering matrix r instead of $\tilde{r}$. From Eq. (12) we realize that this is indeed the case.

Implications.—Our main prediction is that, for purely capacitive coupling between nanotubes, the conductance $G(V)$ into one or both ends of crossed nanotubes must exhibit a structure, as shown in Fig. 2, with a large characteristic "period" $V \sim s/(L\theta)$, where L is the distance from the end to the intersection. Smallness of θ ensures that this structure (envelope in Fig. 2) is distinguishable from size-quantization-like "filling" of the envelope [8,16], which changes with the period $V = \pi s/L$. Also, an important prediction is that the envelope beating structure in Fig. 2 vanishes with temperature much slower than the filling, which vanishes at $T \sim s/L$.

The loop geometry of Ref. [17] offers another possible experimental implication. For this geometry, the easiest way to compare the Sagnac oscillations in Ref. [17] and our finding Eq. (15) is to assume that interaction is weak. Then the contribution to the differential conductance from the Sagnac effect is roughly the product of "size-quantization" oscillations $\propto \cos(2VL/v_F)$ and the envelope $\propto \cos(2VLu_g/v_F^2)$, where V is the source-drain bias, L is the loop perimeter, and u_g is the gate-induced detuning of the "left" and "right" velocities. Our Eq. (15) for this geometry contains the same first cosine $\cos(2VL/v_F)$, while the envelope is entirely due to interactions. Thus, a common feature of the two effects is that envelopes survive at "high" temperatures when Fabry-Perot oscillations vanish.

Concluding remarks.—Adding a second parallel nanotube to a given one leads [18] to a reduction of α in $G(V)$ by a factor of 2. One could expect that, for a finite crossing angle, the effect of the second nanotube is weaker. We found, however, that $G(V)$ depends on θ in a nonanalytical fashion when $\theta \to 0$. This nonanalyticity translates into a peculiar bias dependence of G, as shown in Fig. 2. Thus, for crossed nanotubes, $G(V)$ is extremely sensitive to the value of intratube Luttinger liquid parameter g. In armchair nanotubes, the currently accepted value [1–3] is in the range 0.19–0.26. We emphasize that changing g from 0.19 to 0.26 leads to the increase of the interaction parameter λ by a factor of 2, which would have a drastic effect on the shape of envelope in $\delta G(V)$ (Fig. 2).

Concerning the relation between our study and earlier studies [5,13] of crossed nanotube junctions, this relation is exactly the relation between plasmon and electron scattering. In the above papers, anomalies were either due to direct passage of electrons through the crossing point [13] or due to crossing-induced electron backscattering [5]. Scattering of plasmons was disregarded in Ref. [5]. This is justified for perpendicular nanotubes of Ref. [5]. As shown in this Letter, scattering of plasmons becomes important at small angles.

The work was supported by the Petroleum Research Fund (Grant No. 43966-AC10), DOE (Grant No. DE-FG02-06ER46313), and the Research Corporation (J. M. G.).

[1] M. Bockrath *et al.*, Nature (London) **397**, 598 (1999).
[2] Z. Yao *et al.*, Nature (London) **402**, 273 (1999).
[3] H. Postma *et al.*, Science **293**, 76 (2001).
[4] H. Ishii *et al.*, Nature (London) **426**, 540 (2003).
[5] B. Gao *et al.*, Phys. Rev. Lett. **92**, 216804 (2004).
[6] N. Y. Kim *et al.*, Phys. Rev. Lett. **99**, 036802 (2007).
[7] See the review H. Steinberg *et al.*, Nature Phys. **4**, 116 (2008), and references therein.
[8] C. Kane, L. Balents, and M. P. Fisher, Phys. Rev. Lett. **79**, 5086 (1997).
[9] I. Ussishkin and L. I. Glazman, Phys. Rev. Lett. **93**, 196403 (2004).
[10] M. Fabrizio and A. O. Gogolin, Phys. Rev. B **51**, 17 827 (1995).
[11] A. Komnik and R. Egger, Phys. Rev. Lett. **80**, 2881 (1998).
[12] M. S. Fuhrer *et al.*, Science **288**, 494 (2000).
[13] A. Bachtold *et al.*, Phys. Rev. Lett. **87**, 166801 (2001).
[14] D. L. Maslov and M. Stone, Phys. Rev. B **52**, R5539 (1995).
[15] A. Gramada and M. E. Raikh, Phys. Rev. B **55**, 1661 (1997); **55**, 7673 (1997).
[16] T. V. Shahbazyan, I. E. Perakis, and M. E. Raikh, Phys. Rev. B **64**, 115317 (2001).
[17] G. Refael, J. Heo, and M. Bockrath, Phys. Rev. Lett. **98**, 246803 (2007).
[18] K. A. Matveev and L. I. Glazman, Phys. Rev. Lett. **70**, 990 (1993).